Modeling Pilot-Flight Control System Interactions in the Presence of Uncertainty

Abdullah Habboush* and Yildiray Yildiz†
Bilkent University, Ankara, 06800, Turkey

Despite the numerous advances in control theory over the past decades, humans' versatility in controlling complex systems is still irreplaceable due to their adaptive capabilities. Yet, when it comes to implementing adaptive controllers in piloted applications, unfavorable interactions of human pilots with control systems are observed in certain applications. While several studies exist in the literature that investigate pilot – controller interactions, they are primarily based on linear and fixed dynamics. These studies are useful to study the ideal system behavior, however they may not be helpful in analyzing uncertainties and failures in system dynamics and the adaptive response of the human operator to these undesired occurrences. In this paper, we fill this gap by proposing a closed loop system analysis consisting of adaptive dynamics for both the pilot and the flight control system. This analysis can offer guidance in designing adaptive control architectures to enhance safety measures in real world manned applications.

I. Introduction

The field of mathematical human pilot modeling and the study of human-controller interactions emerged mainly due to the increasing demand for the improvement of aviation safety and handling quality measures. Despite the numerous advances in control theory over the past decades, the human's versatility in controlling complex systems is still irreplaceable due to their adaptive capabilities. Although it is not feasible to model all characteristics of human reactions, many pilot models are proposed in the literature describing different aspects of the human control behavior [1, 2]. These pilot models serve as powerful tools that can be utilized to predict human interactions with the control system and hence provide valuable guidance in the design and optimization of various control architectures.

The crossover model proposed by McRuer [3] is one of the most important pilot models which is derived based on experimental observations that a human operator controls a system in such a way that results in a well-designed linear feedback system. This model along with the quasi-linear model, which includes a linear and a remnant nonlinear term to capture the human's dominant and nonlinear behaviors [4], form the basis from which many extensions are developed to handle a wide range of problems with time-invariant controlled elements. But, when it comes to modeling systems that are prone to failures, damage, and sudden parametric changes, these fixed pilot models fail to resemble how a human is found to respond adaptively in such critical situations. Therefore, since the human is kept in the loop to deal particularly with these unfavorable events, it is of great importance to develop an adaptive human pilot model that can help provide guidance in the design of controllers for such uncertain systems. However, these type of models are rare in the literature due to the difficulty of defining the adaptive nature of the pilots mathematically.

One of the prominent adaptive human pilot models is the one proposed in [5], where the adaption laws are based on expert knowledge. The idea in [5] is to design the adaptive laws in such a way that the pilot model follows the dictates of the crossover model [6]. Inspired by this idea, an experimentally validated adaptive human pilot model is recently proposed in [7] and [8], where the model is developed employing the model reference adaptive control architecture (MRAC), which allows a rigorous stability analysis using the Lyapunov-Krasovskii stability criteria. It is noted that adaptive human pilot studies presented in [5–8] are conducted assuming that the adaptive pilot is facing a linear controller-plant combination. There exist studies such as [9], in which an adaptive controller is in the loop, thus making the controller-plant combination nonlinear and time-varying. However, the pilot model in [9] is linear and time invariant.

The field of adaptive control systems has considerably evolved in the last decades, introducing numerous adaptive control techniques to maintain the stability and performance of a variety of uncertain dynamical systems. The

*A. Habboush is a Graduate Student in the Mechanical Engineering Department and a Member of Systems Laboratory at Bilkent University, Ankara 06800, Turkey (a.habboush@bilkent.edu.tr).
†Y. Yildiz is an Assistant Professor in the Mechanical Engineering Department and the Director of Systems Laboratory (yildirayyildiz.com) at Bilkent University, Ankara 06800, Turkey (yyildiz@bilkent.edu.tr).

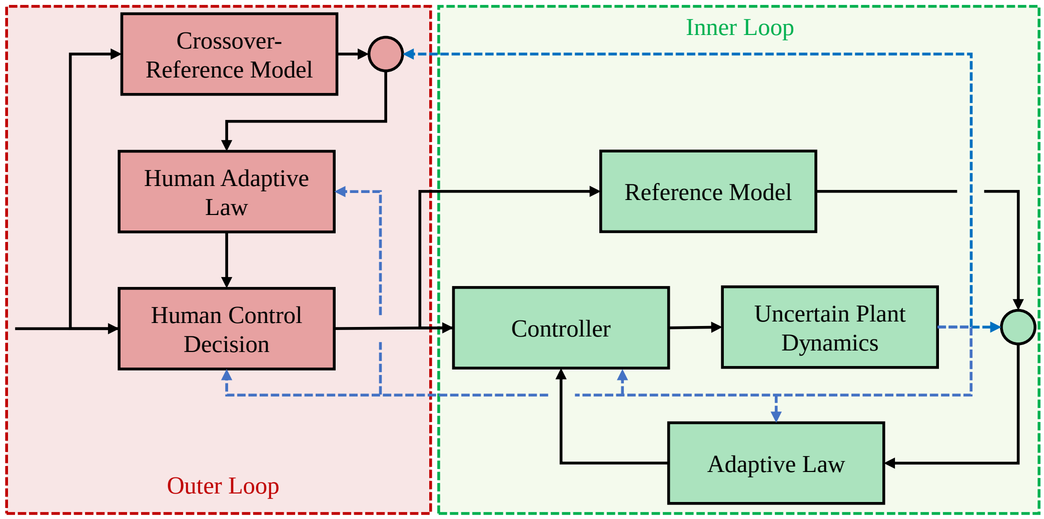

Fig. 1 Block Diagram

implementation of such techniques in several unmanned applications shows improvements in both performance and stability in the face of failure. Yet, when it comes to implementing adaptive controllers in piloted applications, unfavorable interactions of human pilots with the adaptive control systems are observed in several flight tests (e.g., PIOs), owing to the special nonlinear characteristics of adaptive control systems [10].

The study we present in this paper distinguishes itself from the aforementioned results by providing a closed loop system analysis where both the pilot and the flight control system are adaptive, in the presence of uncertain plant dynamics. Although adaptive controllers provide improved stability and performance in unmanned applications, it is known through flight tests that in piloted cases unfavorable interactions can occur between the pilot and the adaptive controller [10]. The aim of this paper is to understand the stability characteristics of adaptive pilot - adaptive controller interactions, paving the way towards a safe implementation of adaptive controllers in real aircraft systems.

We begin with the introduction of the problem statement in Section II. We then present MRAC and adaptive human model architectures in Sections III and IV, respectively. Simulation studies are presented in Section V, and a summary is provided in Section VI.

The notation used here is the standard, where $\mathbb{R}^{p\times q}$ $[\mathbb{S}^{p\times q}]\{\mathbb{D}^{p\times q}\}$ denotes the set of real [symmetric real]{diagonal real} p by q matrices, and $\|.\|$ refers to the euclidean norm for vectors ($q = 1$), and the induced-2 norm for matrices. $\mathrm{Tr}\{.\}$ refers to the trace operator, and $(.)^T[(.)^{-1}]$ denotes the transpose [inverse] operator. Finally, we write $\lambda_{min}(A)$ for the minimum eigenvalue of the matrix A and we denote the set of positive definite real matrices by $\mathbb{R}_+^{p\times p}$.

II. Problem Statement

In the aim of modeling the human's adaptive control behavior in the loop with an adaptive control system, we start with a block diagram given in Fig. 1. In the figure, the block diagram is divided into inner and outer loops. The inner-loop consists of an adaptive controller controlling a plant with uncertain dynamics such that the plant states follow those of a reference model. The reference model is designed to help a specific plant output achieve satisfactory tracking of the human's command.

On the other hand, the outer-loop architecture consists of the human controlling the inner-loop architecture such that a specific plant output follows a reference input fed to the human. The human is assumed to be well trained, i.e, familiar with the nominal plant-controller dynamics. However, he/she is not directly aware of the uncertainties in the plant dynamics. This motivates modeling the adaptive nature of the human as an adaptive outer-loop controller. The crossover-reference model is based on [3].

III. Inner Loop

Consider the following uncertain plant dynamics

$$\begin{aligned}\dot{x}_p(t) &= A_p x_p(t) + B_p u_p(t) + B_p W^T \sigma_p(x_p(t)),\\ y_1(t) &= C_1^T x_p(t),\\ y_2(t) &= C_2^T x_p(t),\end{aligned} \tag{1}$$

where $x_p(t) \in \mathbb{R}^{n_p}$ is the accessible state vector, $u_p(t) \in \mathbb{R}^m$ is the plant control input, $\sigma_p(x_p(t)) : \mathbb{R}^{n_p} \to \mathbb{R}^s$ is a known possibly non-linear basis function, $W \in \mathbb{R}^{s \times m}$ is an unknown weight matrix, $A_p \in \mathbb{R}^{n_p \times n_p}$ is an unknown system matrix, $B_p \in \mathbb{R}^{n_p \times m}$ is a known control input matrix, and $C_1 \in \mathbb{R}^{n_p \times m}$ and $C_2 \in \mathbb{R}^{n_p \times r}$ are both known output matrices. The outputs $y_1(t) \in \mathbb{R}^m$ and $y_2(t) \in \mathbb{R}^r$ are the outputs of interest for the inner and outer loops, respectively. Furthermore, it is assumed that the pair (A_p, B_p) is controllable.

Let the nominal plant dynamics be given as

$$\dot{x}_n(t) = A_n x_n(t) + B_p u_n(t), \tag{2}$$

where $u_n(t) \in \mathbb{R}^m$ is a nominal controller given as

$$u_n(t) = -L_x x_n(t) + L_r y_h(t), \tag{3}$$

where $y_h(t) \in \mathbb{R}^m$ is the human command, and $L_x \in \mathbb{R}^{m \times n_p}$ is selected such that $A_r \triangleq A_n - B_p L_x$ is Hurwitz. It is noted that the human input $y_h(t)$ is bounded due to physical manipulator limits. In the design of the outer loop, given in the following section, human input saturation bounds imposed by the manipulator limits are considered in the stability analysis. Defining $B_r \triangleq B_p L_r$, the reference model is assigned as

$$\dot{x}_r(t) = A_r x_r(t) + B_r y_h(t). \tag{4}$$

For a constant y_h, at steady state, it is obtained using (4) that

$$\dot{x}_r(\infty) = 0 = A_r x_r(\infty) + B_r y_h, \tag{5}$$

and therefore

$$x_r(\infty) = -A_r^{-1} B_p L_r y_h. \tag{6}$$

This means that once the reference model state tracking is achieved, i.e., $\lim_{t\to\infty} x_p(t) = x_r(t)$, the plant output $y_1(t)$, given in (1), takes the form

$$y_1(\infty) = -C_1^T A_r^{-1} B_p L_r y_h. \tag{7}$$

Selecting

$$L_r = -(C_1^T A_r^{-1} B_p)^{-1}, \tag{8}$$

results in $\lim_{t\to\infty} y_1(t) = y_h$.

Considering the uncertain dynamics in (1), let the plant control law be defined as

$$u_p(t) = -\hat{K}_x(t) x_p(t) + L_r y_h(t) - \hat{W}^T(t) \sigma_p(x_p(t)), \tag{9}$$

where $\hat{K}_x(t) \in \mathbb{R}^{m \times n_p}$ and $\hat{W}(t) \in \mathbb{R}^{s \times m}$ are adjustable adaptive parameters serving as estimates for the ideal values K_x^* and W, respectively. It is assumed that the ideal value K_x^* exists such that

$$A_p - B_p K_x^* = A_r. \tag{10}$$

Substituting (9) into (1), one can rewrite (1) as

$$\dot{x}_p(t) = A_r x_p(t) + B_r y_h(t) - B_p \left(\tilde{K}_x(t) x_p(t) + \tilde{W}^T(t) \sigma_p(x_p(t)) \right), \tag{11}$$

where $\tilde{K}_x(t) \triangleq \hat{K}_x(t) - K_x^*$ and $\tilde{W} \triangleq \hat{W}(t) - W$ are the adaptive parameters errors. Defining $\Theta(t) \triangleq [\hat{W}^T(t),\ \hat{K}_x(t)]^T \in \mathbb{R}^{(s+n_p)\times m}$, with the corresponding ideal value $\Theta^* \triangleq [W^T,\ K_x^*]^T$, equation (11) can be rewritten as

$$\dot{x}_p(t) = A_r x_p(t) + B_r y_h(t) - B_p \tilde{\Theta}^T(t) \sigma(x_p(t)), \tag{12}$$

where $\tilde{\Theta}(t) \triangleq \Theta(t) - \Theta^*$ is the lumped adaptive parameter error, and $\sigma(x_p(t)) \triangleq [\sigma_p^T(x_p(t)),\ x_p^T(t)]^T \in \mathbb{R}^{s+n_p}$ is an aggregated known basis function. Subtracting (4) from (12) results in the error dynamics

$$\dot{e}_1(t) = A_r e_1(t) - B_p \tilde{\Theta}^T(t)\sigma(x_p(t)), \tag{13}$$

where $e_1(t) \triangleq x_p(t) - x_r(t)$ is the inner-loop tracking error. We define the adaptive law as

$$\dot{\tilde{\Theta}}(t) = \dot{\Theta}(t) = \gamma_1 \sigma(x_p(t)) e_1(t)^T P_1 B_p, \tag{14}$$

where $\gamma_1 \in \mathbb{R}_+$ is a learning rate, and $P_1 \in \mathbb{R}_+^{n_p \times n_p} \cap \mathbb{S}^{n_p \times n_p}$ is the solution of the Lyapunov equation

$$A_r^T P_1 + P_1 A_r = -Q_1, \tag{15}$$

for some $Q_1 \in \mathbb{R}_+^{n_p \times n_p} \cap \mathbb{S}^{n_p \times n_p}$.

Lemma 1: [Inner-loop stability]

Consider the uncertain dynamical system given by (1), the reference model given by (4), and the feedback control law given by (9) and (14), which can be rewritten compactly as

$$u_p(t) = -\Theta^T(t)\sigma(x_p(t)) + L_r y_h(t). \tag{16}$$

The solution $(e_1(t), \tilde{\Theta}(t))$ is Lyapunov stable in the large. Furthermore, since the human command $y_h(t)$ is bounded,

$$\lim_{t\to\infty} e_1(t) = 0, \tag{17}$$

and $\dot{\tilde{\Theta}}(t)$ remains bounded along with all the signals in the inner-loop.

Proof: Consider the Lyapunov function candidate

$$V_1(e_1(t), \tilde{\Theta}(t)) = e_1^T P_1 e_1 + \gamma_1^{-1} \mathrm{Tr}\{\tilde{\Theta}^T \tilde{\Theta}\}. \tag{18}$$

Differentiating along the trajectories (13) and (14) yields

$$\begin{aligned} \dot{V}_1 =& \dot{e}_1^T P_1 e_1 + e_1^T P_1 \dot{e}_1 + 2\gamma_1^{-1} \mathrm{Tr}\{\tilde{\Theta}^T \dot{\tilde{\Theta}}\} \\ =& -e_1^T Q_1 e_1 - 2 e_1^T P_1 B_p \tilde{\Theta}^T \sigma(x_p) + 2\gamma_1^{-1} \mathrm{Tr}\{\tilde{\Theta}^T \dot{\tilde{\Theta}}\} \\ =& -e_1^T Q_1 e_1 - 2\mathrm{Tr}\{\tilde{\Theta}^T \sigma(x_p) e_1^T P_1 B_p\} + 2\gamma_1^{-1} \mathrm{Tr}\{\tilde{\Theta}^T \dot{\tilde{\Theta}}\} \\ =& -e_1^T Q_1 e_1 \le 0. \end{aligned} \tag{19}$$

Hence, the solution $(e_1(t), \tilde{\Theta}(t))$ is Lyapunov stable in the large.

Equation (4) indicates that the boundedness of $y_h(t)$ implies the boundedness of $x_r(t)$. The latter coupled with the fact that $e_1(t)$ is bounded imply the boundedness of $x_p(t)$, which in turn implies that $(\dot{e}_1(t), \dot{\tilde{\Theta}}(t))$ are bounded. It then follows from Barbalat's lemma that $\lim_{t\to\infty} e_1(t) = 0$. ■

IV. Outer Loop

We now address the outer-loop structure where the human is controlling the inner-loop dynamics given by (12). We assume that the human operating on the system is well-trained. In other words, the human is familiar with the nominal dynamics (2) and (3). Hence, the only unknown in (12) for the outer loop is $\tilde{\Theta}(t)$ which corresponds to fixed uncertainties in plant dynamics and time-varying inner-loop adaptive parameters.

To address command tracking at the outer loop, consider the integral action

$$\dot{x}_c(t) = y_2(t) - r(t) + J\Delta y(t), \tag{20}$$

where $x_c(t) \in \mathbb{R}^r$ is the integrator state, $r(t) \in \mathbb{R}^r$ is the reference input, and $J \in \mathbb{R}^{r\times m}$ is a constant matrix. The term $J\Delta y(t)$ is included to avoid integrator windup, and it only takes action when the human input is saturated. We refer to

[11] and [12] for a detailed discussion about this integral anti-windup approach called the Back-calculation method. Aggregating (12) and (20) results in the augmented dynamics

$$\dot{x}(t) = Ax(t) + BL_r y_h(t) + B_m r(t) - B_m J\Delta y(t) + BH^T(t)\sigma(x_p(t)), \tag{21}$$

where $x(t) \triangleq [x_p^T(t), x_c^T(t)]^T \in \mathbb{R}^n$ is the augmented state vector with $n = n_p + r$,

$$H^T(t) \triangleq -\tilde{\Theta}^T(t) \tag{22}$$

is an unknown time-varying parameter, and

$$A \triangleq \begin{bmatrix} A_r & 0_{n_p \times r} \\ C_2^T & 0_{r\times r} \end{bmatrix} \in \mathbb{R}^{n\times n}, \tag{23}$$

$$B \triangleq \begin{bmatrix} B_p^T & 0_{m\times r} \end{bmatrix}^T \in \mathbb{R}^{n\times m}, \tag{24}$$

$$B_m \triangleq \begin{bmatrix} 0_{r\times n_p} & -I_{r\times r} \end{bmatrix}^T \in \mathbb{R}^{n\times r}. \tag{25}$$

The goal of the human is to control the system such that the plant states follow that of a unity feedback reference model with an open loop crossover model transfer function. We refer to the latter as the *crossover-reference model* (Fig. 1) throughout the rest of the paper. Let the crossover-reference model be given as

$$\dot{x}_m(t) = A_m x_m(t) + B_m r(t), \tag{26}$$

where $x_m(t) \in \mathbb{R}^n$ is the crossover-reference model state vector, and $A_m \in \mathbb{R}^{n\times n}$ is Hurwitz. Let the human control input be defined as

$$v(t) = -\theta_x x(t) - L_r^{-1}\hat{H}^T(t)\sigma(x_p(t)), \tag{27a}$$

$$y_{h_i}(t) = \begin{cases} v_i(t), & \text{if } |v_i(t)| \le y_{o_i}, \\ y_{o_i}\operatorname{sgn}(v_i(t)), & \text{if } |v_i(t)| > y_{o_i}, \end{cases} \tag{27b}$$

where $-\theta_x x(t)$ is the nominal control law that stabilizes the nominal inner-loop dynamics, with the assumption that there exists $\theta_x \in \mathbb{R}^{m\times n}$ such that $A_m = A - BL_r\theta_x$. The term $-L_r^{-1}\hat{H}^T(t)\sigma(x_p(t))$ is the adaptive human input that compensates for the uncertainties in the inner-loop dynamics, where $\hat{H}(t)$ is the estimate of the unknown time-varying parameter $H(t)$. Finally, $y_{o_i} \in \mathbb{R}_+$ is the saturation limit of $y_{h_i}(t)$ (the i^{th} element of $y_h(t)$).

Remark 1: Such a θ_x exists only if A_m is selected such that

$$A_m \triangleq \begin{bmatrix} A_r - B_r\phi & -B_r\psi \\ C_2^T & 0_{r\times r} \end{bmatrix} \in \mathbb{R}^{n\times n}, \tag{28}$$

for some $\phi \in \mathbb{R}^{m\times n_p}$ and $\psi \in \mathbb{R}^{m\times r}$. Then, θ_x can be assigned as

$$\theta_x \triangleq \begin{bmatrix} \phi & \psi \end{bmatrix} \in \mathbb{R}^{m\times n}. \tag{29}$$

Remark 2: The saturation in (27b) is symmetric, though the following procedure applies to asymmetric saturation as well.

Assumption 1: It is assumed that there exists a matrix $J \in \mathbb{R}^{r\times m}$ such that $M \triangleq J\psi \in \mathbb{R}^{r\times r}$ is Hurwitz. Under this assumption, we select such a J in (20) that makes M Hurwitz. This assumption is used in Theorem 1 below.

Substituting (27) into (21), we obtain that

$$\dot{x}(t) = A_m x(t) + B_m r(t) - B\tilde{H}^T(t)\sigma(x_p(t)) + B_\Delta \Delta y(t), \tag{30}$$

where $\tilde{H}(t) \triangleq \hat{H}(t) - H(t)$ is the outer-loop adaptive parameter error, $\Delta y(t) \triangleq y_h(t) - v(t)$, and $B_\Delta \triangleq BL_r - B_m J$. Subtracting (26) from (30) results in the outer-loop error dynamics

$$\dot{e}_2(t) = A_m e_2(t) - B\tilde{H}^T(t)\sigma(x_p(t)) + B_\Delta \Delta y(t), \tag{31}$$

where $e_2(t) \triangleq x(t) - x_m(t)$ is the outer-loop tracking error.

We generate an auxiliary signal $e_\Delta(t)$ as [13, 14]

$$\dot{e}_\Delta(t) = A_m e_\Delta(t) + B_\Delta \Delta y(t), \quad e_\Delta(t_0) = 0, \tag{32}$$

and define an augmented error signal $e_y(t) \triangleq e_2(t) - e_\Delta(t)$ as

$$\dot{e}_y(t) = A_m e_y(t) - B\tilde{H}^T(t)\sigma(x_p(t)), \tag{33}$$

which is in a standard error model form. We propose the adaptive law that is used to update the adaptive parameter $\hat{H}(t)$ as

$$\dot{\hat{H}}(t) = \gamma_2 \text{Proj}\left(\hat{H}(t), \sigma(x_p(t))e_y(t)^T P_2 B\right), \tag{34}$$

where Proj(., .) is the projection operator, [15] $\gamma_2 \in \mathbb{R}_+$ is a learning rate, and $P_2 \in \mathbb{R}_+^{n\times n} \cap \mathbb{S}^{n\times n}$ is the solution of the Lyapunov equation

$$A_m^T P_2 + P_2 A_m = -Q_2, \tag{35}$$

for some $Q_2 \in \mathbb{R}_+^{n\times n} \cap \mathbb{S}^{n\times n}$.

Remark 3: It follows from Lemma 1 that both $\tilde{\Theta}(t)$ and $\dot{\tilde{\Theta}}(t)$ are bounded, which in turn implies the boundedness of the outer-loop uncertainty $H(t)$ and its time derivative $\dot{H}(t)$. Therefore, there exist $h \in \mathbb{R}_+$, and $\dot{h} \in \mathbb{R}_+$ such that $\|H(t)\| \le h$ and $\|\dot{H}(t)\| \le \dot{h}$ for all $t \ge 0$.

Theorem 1: Consider the uncertain dynamical system given by (1), the adaptive controller given by (4),(16) and (14), and the adaptive human pilot model given by (20), (26), (27) and (34). Then, the solution $(e_y(t), \tilde{H}(t))$ remains bounded for all $t \ge 0$ and converges to the compact set

$$E \triangleq \left\{(e_y(t), \tilde{H}(t)) : \|e_y(t)\|^2 \le \eta, \tilde{H}(t) \le \tilde{h}\right\}, \tag{36}$$

where $\eta \triangleq \dfrac{2\gamma_2^{-1}\tilde{h}\dot{h}}{\lambda_{min}(Q_2)}$, and $\tilde{h} \triangleq \|\hat{H}_{max}\| + h$. Furthermore, the closed-loop system is stable in the large, and all signals are bounded.

Proof: Consider the Lyapunov function candidate

$$V_2(e_y(t), \tilde{H}(t)) = e_y^T P_2 e_y + \gamma_2^{-1}\text{Tr}\{\tilde{H}^T\tilde{H}\}. \tag{37}$$

Differentiating along the trajectories (33) and (34) yields

$$\begin{aligned}
\dot{V}_2 =& \dot{e}_y^T P_2 e_y + e_y^T P_2 \dot{e}_y + 2\gamma_2^{-1}\text{Tr}\{\tilde{H}^T\dot{\tilde{H}}\} \\
=& - e_y^T Q_2 e_y - 2e_y^T P_2 B\tilde{H}^T\sigma(x_p) + 2\gamma_2^{-1}\text{Tr}\{\tilde{H}^T\dot{\hat{H}}\} - 2\gamma_2^{-1}\text{Tr}\{\tilde{H}^T\dot{H}\} \\
=& - e_y^T Q_2 e_y - 2\text{Tr}\{\tilde{H}^T\sigma(x_p)e_y^T P_2 B\} + 2\gamma_2^{-1}\text{Tr}\{\tilde{H}^T\dot{\hat{H}}\} - 2\gamma_2^{-1}\text{Tr}\{\tilde{H}^T\dot{H}\} \\
=& - e_y^T Q_2 e_y - 2\gamma_2^{-1}\text{Tr}\{\tilde{H}^T\dot{H}\} \\
&+ 2\text{Tr}\left\{\tilde{H}^T(\text{Proj}\left(\hat{H}(t), \sigma(x_p(t))e_y(t)^T P_2 B\right) - \sigma(x_p(t))e_y(t)^T P_2 B)\right\}.
\end{aligned} \tag{38}$$

Using the projection property $\text{Tr}\{(\theta^T - \theta^{*T})(\text{Proj}(\theta, Y) - Y)\} \le 0$, Remark 2, and Remark 3, we obtain

$$\begin{aligned}
\dot{V}_2 &\le -e_y^T Q_2 e_y - 2\gamma_2^{-1}Tr\{\tilde{H}^T\dot{H}\} \\
&\le -\lambda_{min}(Q_2)\|e_y\|^2 + 2\gamma_2^{-1}\tilde{h}\dot{h}.
\end{aligned} \tag{39}$$

Hence, $\dot{V}_2 < 0$ outside the compact set defined in (36), which proves the boundedness of the solution $(e_2(t), \tilde{H}(t))$, and thus, $\hat{H}(t)$ is also bounded (see Remark 3). The boundedness of all the signals in the inner-loop follow directly from Lemma 1, including $x_p(t)$. According to (26) since $r(t)$ is bounded, $x_m(t)$ is also bounded, which leaves us only to prove that $x_c(t)$ is bounded to complete the proof.

We prove the boundedness of $x_c(t)$ (and hence $x(t)$) by considering the cases where a) $\Delta y(t) = 0$ and b) $\Delta y(t) \neq 0$.

Case a) $\Delta y(t) = 0$.
As $r(t), \tilde{H}(t), y_h(t)$ and $x_p(t)$ are all bounded, it then follows from (30) that $x(t)$ is bounded implying the boundedness of $x_c(t)$.

Case b) $\Delta y(t) \neq 0$.
Consider the integral action (20) rewritten as

$$\dot{x}_c(t) = y_2(t) - r(t) + Jy_h(t) - Jv(t). \tag{40}$$

Substituting (27a), one can rewrite (40) as

$$\dot{x}_c(t) = J\theta_x x(t) + C_2^T x_p(t) - r(t) + Jy_h(t) + JL_r^{-1}\hat{H}^T(t)\sigma(x_p(t)). \tag{41}$$

Using (29), it is obtained by substituting $\theta_x x(t) = \phi x_p(t) + \psi x_c(t)$ into (41) that

$$\begin{aligned}\dot{x}_c(t) =& J\psi x_c(t) + w(t),\\ =& Mx_c(t) + w(t),\end{aligned} \tag{42}$$

where

$$w(t) \triangleq (C_2^T + J\phi)x_p(t) - r(t) + Jy_h(t) + JL_r^{-1}\hat{H}^T(t)\sigma(x_p(t)). \tag{43}$$

As $r(t), \hat{H}(t), y_h(t)$ and $x_p(t)$ are bounded, then so is $w(t)$. Therefore, it follows from Assumption 1 (M is Hurwitz) and equation (42) that $x_c(t)$ is bounded which in turn implies the boundedness of $x(t)$.

The boundedness of $e_2(t)$ follows from the boundedness of $x(t)$ as $x_m(t)$ is bounded, and since $e_y(t) = e_2(t) - e_\Delta(t)$ is bounded, then $e_\Delta(t)$ is also bounded which implies by (32) that $\Delta y(t)$ is bounded and completes the proof. ■

V. Simulations

In this section, we provide an example to demonstrate how the proposed adaptive pilot - adaptive controller modeling framework can be used to test different control variables. For this specific example, we test the effect of adaptive control rates on the human-in-the-loop control system.

Consider the perturbation equations of the longitudinal motion for the 747 airplane [16] cruising in level flight at an altitude of 40 kft and a velocity of 774 ft/sec with the dynamics given in the form of (1), with the state vector

$$x_p(t) = \begin{bmatrix} x_{p1}(t) & x_{p2}(t) & x_{p3}(t) & x_{p4}(t)\end{bmatrix}^T, \tag{44}$$

where $x_{p1}(t)$ and $x_{p2}(t)$ are the components of the aircraft's velocity along the x and z-axes, respectively, with respect to the reference axis (in ft/sec), $x_{p3}(t)$ is the aircraft's pitch rate (in crad/sec), and $x_{p4}(t)$ is the pitch angle of the aircraft (in crad). The input $u_p(t)$ represents the elevator deflection (in crad), and the nominal system and control input matrices are given by

$$A_n = \begin{bmatrix} -0.0030 & 0.0390 & 0 & -0.3220\\ -0.0650 & -0.3190 & 7.7400 & 0\\ 0.0200 & -0.1010 & -0.4290 & 0\\ 0 & 0 & 1 & 0\end{bmatrix}, \quad B_p = \begin{bmatrix} 0.0100\\ -0.1800\\ -1.1600\\ 0\end{bmatrix}, \tag{45}$$

with the eigenvalues at $-0.3750 \pm 0.8818i$ and $-0.0005 \pm 0.0674i$. We consider an uncertainty in the system matrix A_p constructed as

$$A_p = \begin{bmatrix} -0.0029 & 0.0391 & -0.0151 & -0.3234\\ -0.0675 & -0.3214 & 8.0121 & 0.0244\\ 0.0040 & -0.1164 & 1.3243 & 0.1572\\ 0 & 0 & 1 & 0\end{bmatrix}, \tag{46}$$

such that the eigenvalues are placed at 0.1, 0.2, 0.3 and 0.4 in the right-half complex plane. Furthermore, we define the matched system uncertainty by the known basis function $\sigma_p(x_p) = [1,\ x_{p1}(t),\ x_{p2}(t)]^T$ and the unknown weight matrix $W_p = [0.1,\ 0.3,\ -0.3]^T$. A pilot is controlling the aircraft to achieve a desired pitch angle by feeding pitch angle commands to the inner-loop controller, i.e., $y_1(t) = y_2(t) = x_{p4}(t)$, where the pilot command is saturated as in (27b), with $y_o = 30$ deg.

We assign the reference model by designing the nominal controller in (3), where L_x is chosen using the LQR method with $Q_{LQR1} = \text{diag}([0,\ 0,\ 0,\ 5])$, and $R_{LQR1} = 1$. Then, L_r is selected according to (8) to achieve command following at the inner loop. For the outer-loop's human model, the LQR method is used to design the crossover-reference model (26) with $Q_{LQR2} = \text{diag}([0,\ 0,\ 0,\ 0,\ 1.5])$ and $R_{LQR2} = 1$ which yields θ_x in (29) with the sub-matrix $\psi = 1.2247$. Hence, we select $J = -20$ to satisfy Assumption 1. In addition, the Lyapunov matrices are taken as identity matrices for both the inner and outer loops, and the human pilot learning rate is assumed to be $\gamma_2 = 1$.

Figure. 2 shows the tracking performance and the evolution of the pilot command when the inner-loop learning rate $\gamma_1 = 10$. A reasonable tracking performance is observed, while the pilot command shows oscillatory behavior at the initial stages of the scenario. As seen in Fig. 3, when the inner loop learning rate is decreased to $\gamma_1 = 1$, the tracking performance deteriorates. What is more important to observe is that as the flight controller gets slower, the pilot spends more effort, as evident from increased oscillation amplitudes and durations, to be able to fly the aircraft. Finally, Fig. 4 presents the tracking performance and the pilot command curves when the speed of the inner loop is increased to $\gamma_1 = 30$. In this case, pilot activity is dramatically reduced, except the initial oscillatory phase.

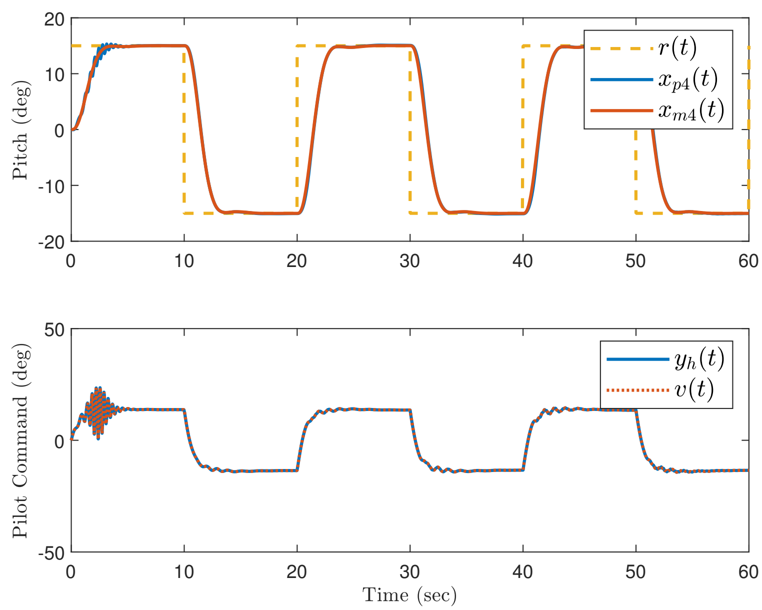

Fig. 2 Results for $\gamma_1 = 10$ and $\gamma_2 = 1$. Top: Reference tracking. Bottom: Pilot command.

The results presented in Figs 2-4 are not geared towards providing high performance controller implementation examples, but rather to demonstrate a use case for the presented modeling approach. It is noted that the results presented here demonstrate only the effect of the flight controller learning rate on the behavior of the pilot. More elaborate studies can be conducted using the proposed framework, such as the selection of reference model parameters, controller initialization, and overall structure of the adaptive controller.

VI. Summary

In this paper, we provide a closed loop system analysis where both the pilot and the flight control system are adaptive, in the presence of uncertain plant dynamics. The analysis has the potential to offer guidance in designing adaptive control architectures when a human pilot is present in the loop. An example system analysis is provided through simulations where it is shown that the selection of the inner loop learning rate can determine the amount of control

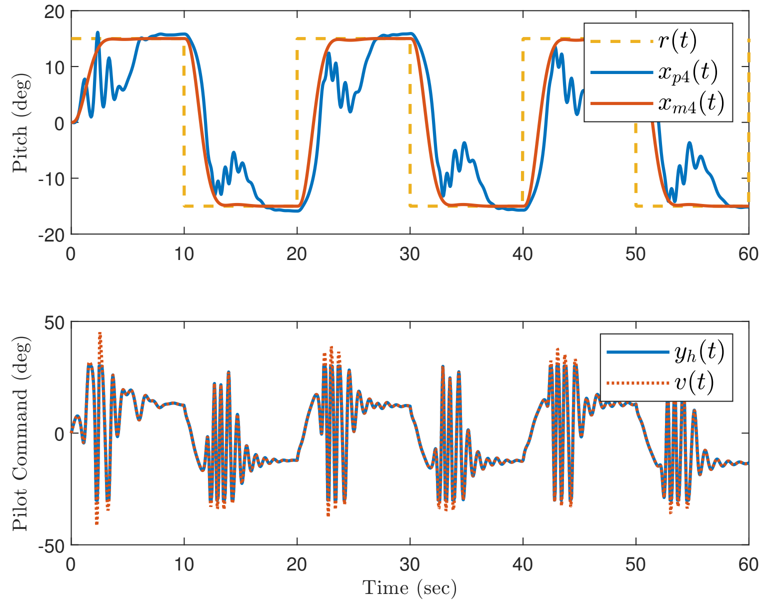

Fig. 3 Results for $\gamma_1 = 1$ and $\gamma_2 = 1$. Top: Reference tracking. Bottom: Pilot command.

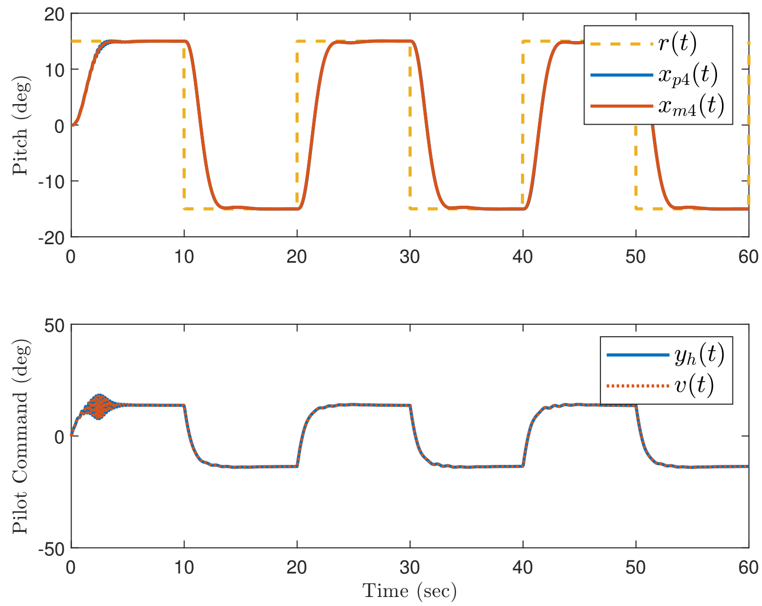

Fig. 4 Results for $\gamma_1 = 30$ and $\gamma_2 = 1$. Top: Reference tracking. Bottom: Pilot command.

effort required by the pilot in the presence of destabilizing uncertainty and control effectiveness reduction.

References

[1] Lone, M., and Cooke, A., "Review of pilot models used in aircraft flight dynamics," *Aerospace Science and Technology*, Vol. 34, 2014, pp. 55–74.

[2] Xu, S., Tan, W., Efremov, A. V., Sun, L., and Qu, X., "Review of control models for human pilot behavior," *Annual Reviews in Control*, Vol. 44, 2017, pp. 274–291.

[3] McRuer, D., and Graham, D., "Pilot-vehicle control system analysis," *Guidance and Control Conference*, 1963, p. 310.

[4] McRuer, D. T., and Jex, H. R., "A review of quasi-linear pilot models," *IEEE transactions on human factors in electronics*, , No. 3, 1967, pp. 231–249.

[5] Hess, R. A., "Modeling pilot control behavior with sudden changes in vehicle dynamics," *Journal of Aircraft*, Vol. 46, No. 5, 2009, pp. 1584–1592.

[6] Hess, R. A., "Modeling human pilot adaptation to flight control anomalies and changing task demands," *Journal of Guidance, Control, and Dynamics*, Vol. 39, No. 3, 2016, pp. 655–666.

[7] Tohidi, S. S., and Yildiz, Y., "A Control Theoretical Adaptive Human Pilot Model: Theory and Experimental Validation," *arXiv preprint arXiv:2007.10216*, 2020.

[8] Tohidi, S. S., and Yildiz, Y., "Adaptive human pilot model for uncertain systems," *2019 18th European Control Conference (ECC)*, IEEE, 2019, pp. 2938–2943.

[9] Yucelen, T., Yildiz, Y., Sipahi, R., Yousefi, E., and Nguyen, N., "Stability limit of human-in-the-loop model reference adaptive control architectures," *International Journal of Control*, Vol. 91, No. 10, 2018, pp. 2314–2331.

[10] Klyde, D., Liang, C.-Y., Alvarez, D., Richards, N., Adams, R., and Cogan, B., "Mitigating unfavorable pilot interactions with adaptive controllers in the presence of failures/damage," *AIAA Atmospheric Flight Mechanics Conference*, 2011, p. 6538.

[11] Astrom, K. J., and Rundqwist, L., "Integrator windup and how to avoid it," *1989 American Control Conference*, IEEE, 1989, pp. 1693–1698.

[12] Kapoor, N., Teel, A. R., and Daoutidis, P., "An anti-windup design for linear systems with input saturation," *Automatica*, Vol. 34, No. 5, 1998, pp. 559–574.

[13] Karason, S. P., and Annaswamy, A. M., "Adaptive control in the presence of input constraints," *1993 american control conference*, IEEE, 1993, pp. 1370–1374.

[14] Schwager, M., and Annaswamy, A. M., "Direct adaptive control of multi-input plants with magnitude saturation constraints," *Proceedings of the 44th IEEE Conference on Decision and Control*, IEEE, 2005, pp. 783–788.

[15] Lavretsky, E., and Wise, K. A., "Robust adaptive control," *Robust and adaptive control*, Springer, 2013, pp. 317–353.

[16] Bryson, A. E., *Control of spacecraft and aircraft*, Princeton university press, 1994.